Preliminary investigation into the function of *tfap2a* transcript variants in zebrafish development

Thanh Bao Dan Nguyen, Jessica Patrick, Vida Senkus Melvin

Department of Biology, Metropolitan State University of Denver, CO 80204, USA

Abstract

The transcription factor AP2α (*tfap2a*) has been identified as an important regulator of neural crest cell (NCC) development. NCC are a multipotent stem cell population that differentiates to many cell types, including melanocytes and craniofacial cartilages. Disruption of *tfap2a* leads to defects in NCC-derived cell types in many organisms. In zebrafish, mutations in *tfap2a* results in *lockjaw* (*low*) and *mont blanc* phenotypes with severe reduction in body melanocytes and defects in cartilages of the second/hyoid arch. There are three highly conserved *tfap2a* transcript variants that differ at 5' exon 1, called V1a, V1b, and V1c. Despite their high conservation across species, their functions in development are still elusive. In this project, we investigate the roles of these variants in zebrafish development, using splice-blocking morpholinos that disrupt variant splicing and expression individually. Our preliminary data demonstrated that only disruption of V1b results in reduced melanocytes and cartilage defects similar to *low* mutants, while morphants with V1a disruption showed no phenotypes, and disruption of V1c only induces melanocyte reduction. These data suggest that V1b is the functional *tfap2a* transcript variant in NCC development, while V1c may only contribute to NCC-derived melanocyte development and V1a may not be functional in NCC-development at all. These data are promising; however, future experiments are needed to confirm the phenotypes induced by disruption of *tfap2a*-specific variants. In conclusion, this project is the first one that examines the function of these *tfap2a* variants in development.

Introduction

The vertebrate jaw, head, and facial skeleton are mainly derived from neural crest cells (NCC), a population of multipotent stem cells that arises from the dorsal edge of neural folds during neural tube closure (Mayor and Theveneau, 2013). Most of the craniofacial skeleton originates from the cephalic or cranial NCC, which emerges at the neural folds from the diencephalon to the third somite (Mayor and Theveneau, 2013). In all vertebrates, cranial NCC migrate either along the anteroposterior (A-P) axis or the mediolateral axis and contribute to the formation of many different cell types, including cartilage forming cells in the pharyngeal arches and pigment cells (Theveneau and Mayor, 2012). Patterning of these arches has been demonstrated to be highly conserved among different species despite differences in shape and number of arch-derived skeletal elements (Mork and Crump, 2015). For example, NCC in the mandibular or first arch forms the jaw in fish and corresponds to the lower jaw of humans, parts of the mammalian pharynx, and the inner ear bones, incus and malleus. Meanwhile, NCC migrating into the hyoid or second arch forms the gill-bearing viscerocranium

in fishes and corresponds to the stapes, another structure of mammalian inner ear bones (Mork and Crump, 2015). These similar structures suggest a shared gene network and mechanism in NCC development across different species.

Among many molecules in the complex NCC gene network, the transcription factor AP-2α *(tfap2a*) has been identified as a critical mediator of NCC development. Early studies have demonstrated that disruption of *tfap2a* results in defects of multiple NCC-derived cell types. For instance, loss of *tfap2a* in mice resulted in severe craniofacial defects, including exencephaly and cleft palate, defects in middle ear ossicles, and failure of neural tube closure that resulted in death before or shortly after birth (Zheng *et al*., 1996, Brewer *et al., 2004*). In zebrafish, mutations in *tfap2a,* characterized in the *lockjaw* (*low*) and *mont blanc* (*mob*) mutants, showed reduced body melanocytes (pigment cells) and craniofacial defects, especially in cartilages derived from the second arch (Knight *et al*., 2003, Barrallo-Gimeno *et al*., 2004). Further analysis in *tfap2a* zebrafish mutants showed that NCC were induced and migrated properly to their destinations, but upon their arrival, failed to survive and differentiate sufficiently into their lineage cell types (Barrallo-Gimeno *et al*., 2004, Knight *et al*., 2003). Other studies also demonstrated that *tfap2a* is required for proper expression of melanocyte differentiation genes and transcription of Hox group 2 genes, which induce segmental identities of NCC at the second/hyoid arch (Knight *et al*., 2004, Seberg *et al*., 2017). The similar phenotypes between *tfap2a* mutants in mice and zebrafish indicate conserved functions of this transcription factor in vertebrate NCC development.

The *tfap2a* gene is composed of seven exons, which encode a highly conserved, basic helix-span-helix DNA-binding domain (exons 4-7; Figure 1A) and an amino-terminal, proline/glutamine-rich trans-activation domain (exon 2; Figure 1A; Williams and Tijian, 1991a, William and Tjian, 1991b, Eckert *et al.,* 2005). Several *tfap2a* transcript variants have been identified, but there are three variants called variants 1a, 1b, and 1c that are highly conserved across vertebrates (Figure 1A; V1a, V1b, V1c). These transcript variants have alternative exon 1 at the 5' end and share exons 2 through 7, which encode the DNA-binding and transactivation functions (Figure 1A). Each alternative exon 1 encodes at least one possible initiator methionine and short sequences of unique amino acids at the N-terminus of the protein (Meier *et al.,* 1994, Berlato *et al.,* 2011; Figure 1). Alignment between homologs of these three variants in zebrafish, mice, and human demonstrated their high conservation across different species. Human, mouse and zebrafish *tfap2a* transcript variant sequences show nearly 100% identity in the amino acids encoded by exon 1 (Figure 1). The conservation of these *tfap2a* variants across different species suggests that they carry important functions in normal development and

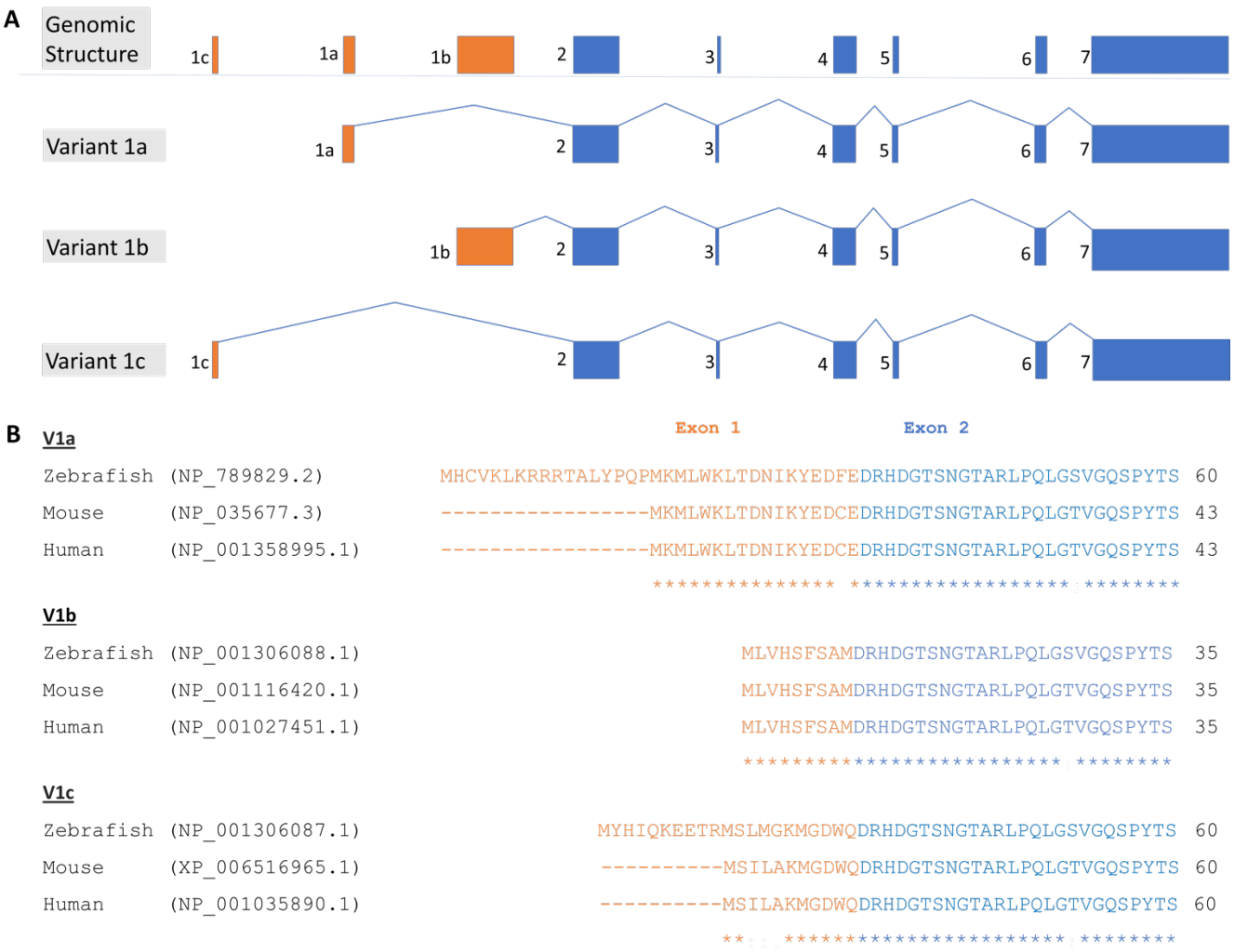

Figure 1. (A) Genomic structure of *tfap2a* with exons depicted as boxes and introns as lines. The exon structure of the three conserved 5'-transcript variants are also shown, each with a unique exon 1 (orange) and shared exons 2-7 (blue). (B) Variant specific amino acids from human, mouse, and zebrafish were compared using Clustal Omega Multiple Sequence Alignment using exon 1 encoded sequences starting at the mapped start codon for humans. There is an in-frame, upstream start codon in zebrafish for V1a and V1c, but there are no published data to indicate which AUG is used. Amino acid sequences that are unique to each variant are colored orange, while common exon 2 encoded sequence is indicated in blue. All three variants show a high degree of identity – Variant 1a (94%), Variant 1b (97%), and Variant 1c (82%). NCBI refseq IDs are provided for peptide sequences. Asterisks (*) indicates position that share identity in all here species.

have been preserved over time (Berlato *et al*., 2011). Therefore, understanding their function and expression will enable a better understanding of the role of *tfap2a* in NCC development.

Despite their conservation across species, the role of these *tfap2a* variants during development has not been investigated. Previous knock-out experiments targeted more 3'-exons of *tfap2a* and affect all three 5'-transcript variants (Knight *et al.,* 2003, Knight *et al.*, 2004, Brewer *et al.,* 2004). Thus, these previous studies do not enable analysis of the function of each 5'-variant individually. In this project, we examine the function of *tfap2a* variants in zebrafish development using variant-specific morpholinos to disrupt expression of each 5'-transcript individually. The resulting phenotypes were examined for changes in NCC-derived cells and

structures, including melanocyte development and formation of craniofacial cartilages, using the well-characterized *low* phenotype as the standard for analysis. This project is the first to investigate the functions of individual *tfap2a* transcript variants during development.

Materials and Methods

Zebrafish Strains

Adult zebrafish of the genetic line AB (offspring of the original A and B genetic lines established in the 1970s) were obtained from the Zebrafish International Resource Center (ZIRC, Eugene, Oregon). These fish are maintained on a housing apparatus similar in design to that outlined in (Kim *et. al*, 2009).

Morpholinos

Morpholinos (MO) were designed by Gene-Tools (Philomath, OR) to the unique exon 1-intron 1 splice junction of *tfap2a* 5'-transcript variants (Figure 1A). MO sequences are as follows: V1a AAGCCGCTTACCTCGAAGTCTTCAT, V1b ACTCC-CGACATTCACTCACCATCGC, and V1c AGGAAGAGAACGTACCTGCCAGTCT. As a positive control, we also used the 5.1 MO CCTCCATTCTTAGATTTGGCCCTAT, which binds at the exon 5-intron 5 junction of *tfap2a* (Knight *et al.*, 2003). Morpholinos were resuspended in nuclease free water to a concentration of 1mM before auto injected at the one cell stage with a Drummond Nanoject II injector. Embryos that are injected with MO are called "morphants" to distinguish them from uninjected wildtype embryos.

A dose of 5ng MO was injected with 2.5% fluorescein (Item #D1820, ThermoFischer Scientific) as a tracer for 5.1, V1a, and V1b. Injection with the V1c MO at 5ng induced embryonic lethality or phenotypes including edema of the yolk and heart, as well as smaller heads (data not shown). These phenotypes are not an anticipated outcome of *tfap2a* knock-down (Knight *et al.*, 2003 and Barrallo-Gimeno *et al*., 2004). Hypoplasia or underdevelopment of the craniofacial cartilages was observed in the surviving 5ng V1c morphants (data not shown), but these morphants did not show cartilage fusions consistent with the described *low* phenotype (Knight *et al.*, 2003 and Figure 2). Heart and yolk edema and small heads are hallmarks of MO toxicity (Bedell *et al*., 2011*).* Reducing the dose of MO to 2.5ng reduced embryo toxicity and these embryos were used in our analysis. MO toxic embryos were excluded. A minimum of two or three rounds of injections were performed for each morpholino to build data sets.

Phenotype Analysis

After injection, embryos were cultured at 28°C in embryo media and screened at two timepoints, 32 hours post fertilization (hpf) for melanocyte reduction and 5 days post fertilization (dpf) for craniofacial cartilages. Disruption of melanocytes is the earliest visible sign of NCC disruption and are fully observable at 32 hpf when survivability is also documented. Live embryos were scored for

melanocyte reduction and photographs were taken under 5x magnification using a Zeiss Stemi 508 dissection microscope with an Axiocam 105 color camera. Digital photographs were taken and stored using the ZEN 2.3 lite software at 5x magnification. Cartilage structures start to form at 2.5 dpf and are fully developed at 5dpf when zebrafish embryos were fixed and cartilage stained with Alcian blue (Walker & Kimmel, 2007). Stained embryos were stored at 4°C in 50% glycerol 0.1% KOH for phenotype analysis. The neurocranium (NC) and viscerocranium (VC) were separated by dissection using 0.1 x 0.06mm tipped forceps (Item #11251-20, finescience.com). Separation is necessary to fully view the VC, which houses the arch 2 cartilages that are under investigation, while the NC is unaffected by our injections. After dissection, cartilages were flat mounted on glass slides. Photographs of dissected cartilages were taken on an Olympus bx41 microscope with an Olympus DP72 camera at 10X magnification. Cellsense Standard software was used to take and store photographs.

Results

To evaluate the individual function of the *tfap2a* transcript variants *in vivo*, we used antisense morpholinos (MO). MOs function to knockdown gene activity by complementary binding to targeted mRNAs to disrupt splicing and alter protein translation (Stainier *et al*, 2017). The MOs used in this experiment were targeted to the unique exon 1-intron 1 splice junction of each 5'-transcript variant. These "splice" MO disrupt transcript splicing by obstructing the splicing machinery (Schulte-Merker and Stainier, 2017). MO-injected embryos, or morphants, were compared to wild-type, uninjected siblings as a negative control. Effects on NCC-derived cells and structures were evaluated, including approximate number and pattern of melanocytes, and development of craniofacial cartilages (Figure 2A-D). During normal zebrafish development, melanocytes extend from around the eye, along the dorsal aspect of the embryo, with a low density or melanocytes around the eye and a higher density posterior to the otic vesicle at 32hpf (Figure 2A). The cranial cartilages of the zebrafish larvae are apparent as early as 3dpf, and at 5dpf consist of a dorsal neurocranium (not shown) and a ventral viscerocranium (Figure 2C), which is derived from the pharyngeal arches (Mork and Crump, 2015). Pharyngeal arch 1 gives rise to the Meckel's (m) and palatoquadrate (pq) cartilages of the lower jaw. More posterior cartilages derived from pharyngeal arch 2 and 3 contribute to the gill-forming structures and include the hyosymplectic (hs), ceratohyal (c), the small interhyal (ih), and ceratobranchials (cb1-5; Figure 2B-D).

As a positive control for *tfap2a* disruption, we compared *tfap2a* variant morphants to embryos injected with the 5.1 MO, which binds to the exon 5 - intron 5 junction and would disrupt the splicing of all three *tfap2a* variants (Figure 2E-H; Knight *et*

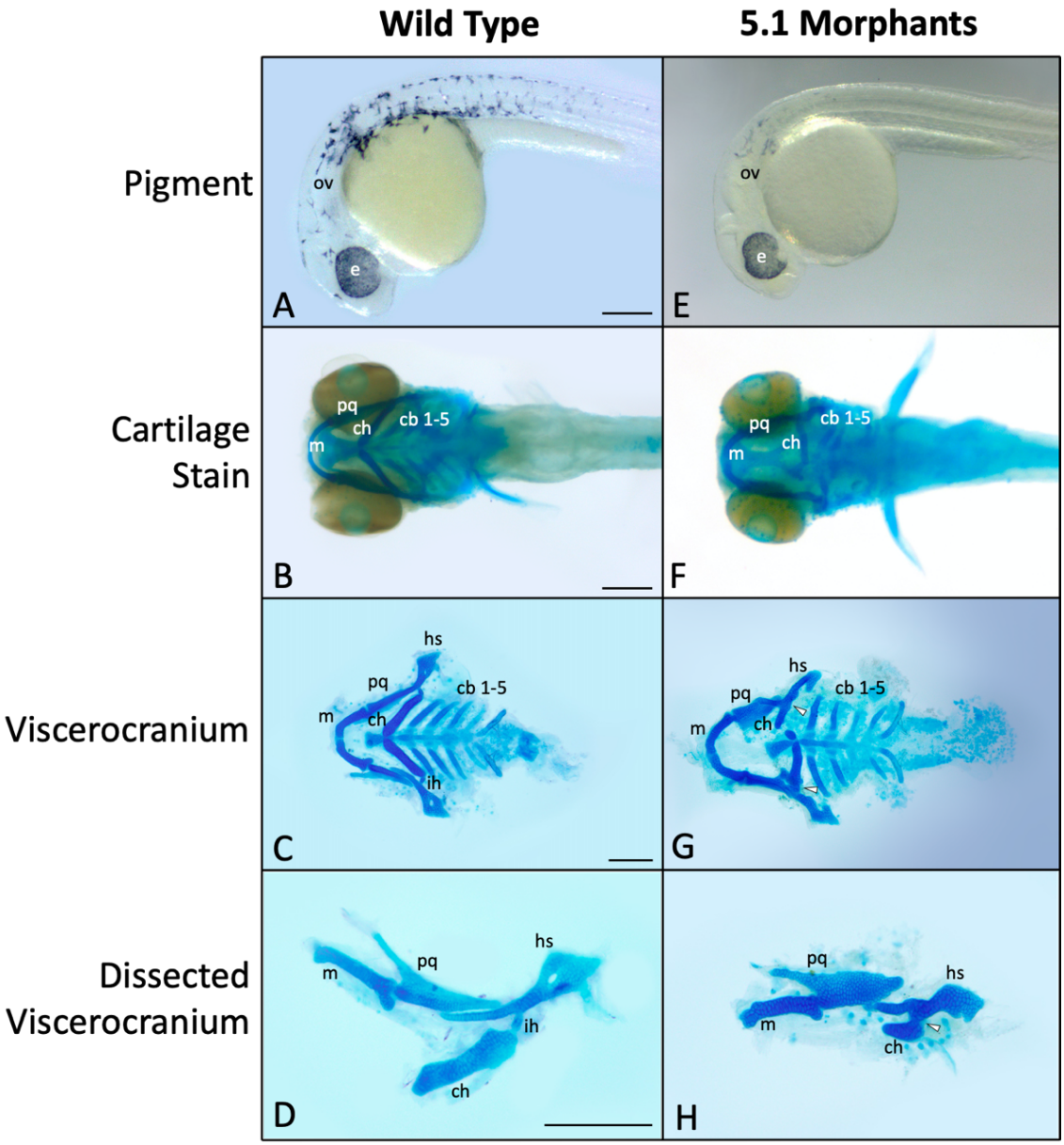

Figure 2. Comparison of uninjected embryos to 5.1 morphant siblings. Lateral views (A,E) of 32hpf embryos show severely reduced melanocytes in 5.1 morphants compared to uninjected (B,F) Ventral views of 5dpf embryos stained with Alcian Blue for cartilage. (C,G) Ventral views of dissected viscerocranium at 5dpf. (D,H) Lateral views of the dissected viscerocranium. Arch 2 cartilages are severely reduced in 5.1 morphants. The fusion between the ceratohyal, hyosymplectic, and interhyal is denoted with arrows in G and H. m, Meckel's; pq, palatoquadrate; ch, ceratohyal; hs, hyosymplectic; ih, interhyal; cb1-5, ceratobranchials 1-5: ov, otic vesicle; e, eye. Size bars are 200μm.

al., 2003). The phenotype of 5.1 morphants has been shown to phenocopy (produce a phenotype that appears nearly identical to) a genomic disruption of *tfap2a*, such as in the *low* and *mob* mutants (Knight *et al.*, 2003 and Barrallo-Gimeno *et al.*, 2004). Injection of the 5.1 MO led to at least a 50% reduction in melanocytes compared to wild type at 32 hpf (Figure 2E) and severely reduced cranial cartilage formation at 5dpf (Figure 2F and G). In 5.1 morphants, the hyoid arch cartilages were consistently inverted or severely reduced or hypoplastic, while the ceratobrachial structures

Table 1. Summary of NCC phenotypes in *tfap2a* morphant embryos

	MELANOCYTE PHENOTYPES		CRANIOFACIAL CARTILAGE PHENOTYPES		
	Normal	Severe	Normal	*Low* phenocopy	Severe
Uninjected	255/285 89.5%	30/285 10.5%	68/76 89.5%	2/76 2.6%	6/76 7.9%
5.1 MO	4/46 9.7%	42/46 91.3%	1/21 4.8%	20/21 95.2%	0/21
V1a MO	117/130 90%	13/130 10%	82/94 87.2%	3/94 3.2%	9/94 9.6%
V1b MO	17/179 9.5%	162/179 90.5%	6/49 12.2%	39/49 79.6%	4/49 8.2%
V1c MO	28/65 43.1%	37/65 56.9%	35/41 85.4%	0/41	6/41 14.6%

are present but appear disorganized (Figure 2G). Reduction of these arch 2 cartilages causes the mandibular structure to collapse, pulling the mouth of the 5dpf larvae ventrally (data not shown). Dissections of the viscerocranium in 5.1 morphants show reduced and partially inverted ceratohyals (95%, Table 1, Figure 2G). In most cases, the ceratohyals are fused directly to the reduced hyosymplectic (arrowhead in Figure 2G and H), while the interhyal is either missing or possibly also fused. Arch 1 derived Meckel's and palatoquadrate cartilages appear largely normal. Loss of melanocytes and a reduction of arch 2 cartilages with cartilage fusions have been reported in *low* mutants and have been consistently replicated through injection of 5.1 MO (Knight *et al.*, 2003). The combination of >50% reduction in pigment and the specific cartilage defects described above copy the *low* phenotype and will be referred to as a "*low* phenocopy" from here on.

Injection of splice-blocking MO to individual *tfap2a* transcript variants produced variable effects on melanocytes (Figure 3A, E, and I). V1a morphants largely displayed melanocyte number and distribution consistent with uninjected embryos (90% Table 1, compare Figure 3A with Figure 2A). In contrast, V1b morphants show an almost complete loss of melanocytes similar to the phenotype in 5.1 morphants (90.5% Table 1, Figure 3E). Melanocytes that are present in V1b morphants

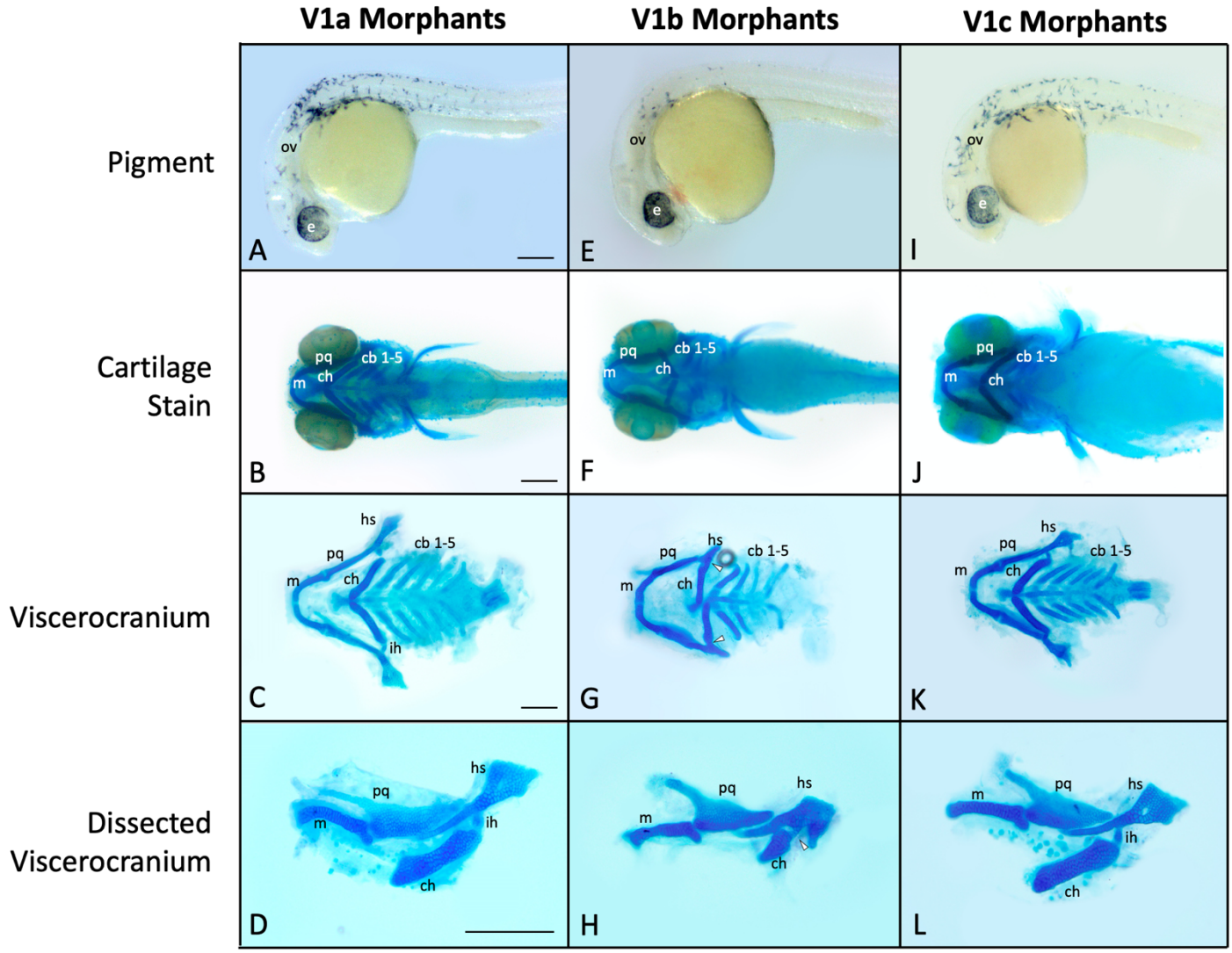

Figure 3. Comparison of V1a, V1b, and V1c morphants. Lateral views (A,E, and I) of 32hpf embryos show melanocytes patterns. (B,F, and J) Ventral views of 5dpf embryos stained with Alcian Blue for cartilage. (C,G, and K) Ventral views of dissected viscerocranium at 5dpf. (D,H, and L) Lateral views of the dissected viscerocranium. Arch 2 cartilages are severely reduced in V1b morphants. The fusion between the ceratohyal, hyosymplectic, and interhyal is denoted with arrows in G and H. Arrows present in G and H denote fusion points in the hyoid joint between the ceratohyal, interhyal, and hyosymplectic. m, Meckel's; pq, palatoquadrate; ch, ceratohyal; hs, hyosymplectic; ih, interhyal; ov, otic vesicle; e, eye. Size bars are 200μm.

appear posterior to the otic vesicle and resemble the pattern observed in 5.1 MO (compare Figure 2E to Figure 3E, Table 1). V1c morphants show variable effects on melanocyte number and pattern, with more than half of morphants displaying a severe reduction in melanocytes (56.9%) and remaining morphants displaying melanocyte patterns similar to uninjected. (Figure 3I, Table 1).

We classified cranial cartilage phenotypes into three categories; "Uninjected", which show the same pattern as uninjected embryos (Figure 2B-D); "*low* phenocopy", which show phenotypes consistent with 5.1 morphants (Figure 2F-G); and "severely affected" embryos, which had phenotypes much more severe than expected showing yolk and heart edema accompanied by malformation and hypoplasia of both arch 1, arch

2, and arch 3-derived cartilages (Table 1 and data not shown). V1a and V1c morphants largely resembled uninjected embryos with no obvious loss or deformation of the cartilage structures (Compare Figure 2 to Figure 3B-D and J-L, Table 1). V1b morphants displayed the most *low* phenocopy morphants with 80% of injected embryos displaying malformation of arch 2 cartilages (Figure 3F-H compared to Figure 2F-H and Table 1). The fusion that is the hallmark of the *low* phenotype in which the ceratohyal, interhyal, and hyosymplectic become fused together is visible in only in V1b morphants (Figure 3G-H compared to Figure 2G-H. Fusion is denoted with an arrowhead).

Discussion

This project investigated the functions of three highly conserved *tfap2a* transcript variants in zebrafish development using variant-specific MOs that inhibit splicing and expression of each transcript individually. Our preliminary data demonstrate that only disruption of *tfap2a* transcript variant V1b phenocopies previously published *tfap2a* mutants, such as *low.* V1b morphants show a 50% reduction in melanocytes and reduction, loss, or fusion of craniofacial cartilages derived from pharyngeal arch 2. Neither disruption of V1a or V1c induced defects in arch 2 craniofacial cartilages similar to the *low* mutant. Disruption of V1c did produce a severe reduction of melanocytes in 57% of the morphants, while V1a showed no melanocyte defects. These data suggest that V1a is not functional in NCC during zebrafish development. On the other hand, V1c and V1b might both contribute to melanocyte development, but only V1b is the functional *tfap2a* transcript variant in NCC-derived craniofacial cartilage development. Though these data are promising, we interpret these data with caution. We do not have evidence that the splice MOs are disrupting splicing. Future experiments utilizing Reverse-Transcriptase Polymerase Chain Reaction (RT-PCR) are necessary to confirm splicing disruption in morphants. More specifically, an increase in the size of the PCR product from morphants would be expected due to retention of intron 1 in the mature mRNA. If we can show that the splice MOs used in this study disrupt splicing, these phenotype data would be the first to demonstrate a functional difference between the 5'-*tfap2a* transcript variants during development.

The presence of alternative first exons in the transcript variants suggests alternative promoter usage, which could lead to different expression patterns in different cell types and developmental stages (Davuluri *et al*., 2008). There is no single study that directly compares the expression of all three 5'-*tfap2a* transcript variants during development. Our lab has begun to investigate the expression of the variants during zebrafish development using RT-PCR. Preliminary data suggest that V1a and V1b are the predominant 5'-transcript variants at all developmental stages being tested (Frazer, Raykovitz, and Melvin,

unpublished data). The V1a and V1b transcripts are more highly expressed than V1c and appear to be approximately equal in expression at each timepoint. This finding suggests that V1a and V1b may have equally important and similar functions in during development, but our morphant phenotypes do not support this idea. In fact, only the disruption of V1b resulted in a phenotype similar to 5.1 morphants and *low*. The lack of phenotype in V1a morphants is surprising given the high expression of V1a during early development. Differences in spatial and cell-type specific expression might account for the functional differences between V1a and V1b *tfap2a* variants during development. For instance, it is possible that V1b is expressed in NCC, while V1a is not. We have attempted *in situ* hybridization studies to examine spatial expression of *tfap2a* isoforms, but the probes to detect only the 5'-ends of each individual transcript are too small to achieve probe specificity and stability (Darnell *et al*., 2010).

Other studies in mouse embryos compared and showed differences in V1a and V1b spatiotemporal expression. At early developmental stages, V1b is the predominant variant but remains at similar or lower level than V1a at later points (Meier *et al.*, 1995). The same study also found that V1b was more dominant in the central and peripheral nervous system, while V1a was more highly expressed in the epidermis (Meier *et al*., 1995). In another study using RT-PCR, V1a showed stronger expression than V1b in embryonic murine lens, which is an epidermally-derived structure, and both variants were equally expressed in kidney, cerebellum, and to a lesser extent, cerebrum and lung (Ohtaka-Maruyama *et al*., 1998). While its spatiotemporal distribution during development is still unknown, V1c expression has been identified in human and ovine placenta, where this variant functions as a trans-activator (Limesand and Anthony *et al*., 2001). Comparison of these *tfap2a* 5'-transcript variants in normal breast tissues and breast cancer cell lines demonstrated that V1a is the predominant transcript, while V1c seems to be more dominant at the protein level, suggesting a potential difference in their post-transcriptional regulation (Berlato *et al*., 2011). None of these studies directly compared all three variants, nor has NCC expression been reported. Studies to examine the spatiotemporal expression the 5'-*tfap2a* variants will be critical to addressing this question.

The use of alternative first exons in the *tfap2a* transcript variants produces AP-2α protein isoforms with small differences in N-terminal amino acids, which could alter protein function. Even though these AP-2 α isoforms share the same DNA-binding and transactivation domains, the small difference in amino acid composition could potentially modify their DNA-binding and transactivation activity. There is no previous study comparing DNA-binding by these isoforms. Studies in normal breast tissues and cell lines found that the three isoforms use the same

coactivators of *tfap2a*, including CBP and p300 (Berlato *et al.,* 2011*)*. However, the authors also found that transactivation activity between the isoforms was significantly different on a known AP-2 α target promoter, ERBB2, with V1a having the lowest activity (Berlato *et al.,* 2011*)*. Comparison of transactivation by the three isoforms on the promoter of the long non-coding RNA HIPSTR found no difference in activity (Yunusov *et al.*, 2016*)*. These published data suggest that functional differences between AP-2 α isoforms in transactivation could be promoter-specific, e.g., these variants behave differently toward different promoters.

In conclusion, only disruption of the V1b transcript variant of *tfap2a* phenocopies the *low* phenotype in our study. These data along with its high expression during early development suggest an important role for this transcript variant in NCC development. On the other hand, these data are preliminary and further experiments are needed to fully examine the function of the V1a and V1c transcript variants in zebrafish development. During the preparation of this manuscript, Chambers *et al.* (2019) characterized a novel *tfap2a* zebrafish mutant called *terminus* (*trm*) that results from a disruption in splicing of V1c. Few details on craniofacial development were provided in these mutants as kidney development was the focus of their study, but they did show a defect of the hyoid cartilage, as well as mild phenotypes in Meckel's cartilage that had not been previously characterized in *low* or *mob* mutants (Chambers *et al*., 2019). These results are intriguing, and it would be interesting to re-examine our V1C morphants more closely to look for similar changes to Meckel's cartilage. We do not see changes to the hyoid cartilage similar to those reported for *trm*, nor did Chambers, et al. indicate whether the *trm* mutants have cartilage fusions characteristic of *low* mutants.

To address these questions, the CRISPR-Cas9 system could be used as an alternative approach to knockdown each individual *tfap2a* variant for gene editing. This method targets the genomic DNA rather than RNA transcripts, thus inducing a stable loss-of-function of each 5'-tfap2a variant individually (Schulte-Merker and Stainier, 2014). Alternatively, the CRISPR/Cas9 system could also be used to produce a "knock-in/knock-out" mutant. Using this method, we could insert a reporter gene, such as a fluorescent protein or *lacZ*, into the exon 1 sequence for each variant. The reporter gene would be under the transcriptional control of the promoter for each variant and would be in-frame with the start codon (AUG). The stop codon for the reporter would prevent translation of the remaining *tfap2a* coding sequence and truncate the protein, leading to a functional knock-out of the individual variant. The reporter gene could also serve as a marker to examine the spatial expression of targeted variants circumventing problems using short probes for in situ hybridization. Even though these data are preliminary and future experiments are still needed, this project is the first to compare the

function of these three highly conserved *tfap2a* transcript variants during development.

Acknowledgments: The authors would like to acknowledge Ashley Raykovitz and Cassie Frazer for their work in analyzing variant expression with RT-PCR. We would also like to thank the Colorado-Wyoming Alliance for Minority Participation (CO-WY AMP) for providing research funding to T.N. and J.P and the College of Letters, Arts, and Science Dean's Mini Grant.

Authors' contributions: Thanh Nguyen and Jessica Patrick contributed equally to this work.

References

Barrallo-Gimeno, A., Holzschuh, J., Driever, W., & Knapik, E. (2004). Neural crest survival and differentiation in zebrafish depends on *mont blanc/tfap2a* gene function. *Development*, *131*(7), 1463–1477.

Bedell, V., Westcot, S., & Ekker, S. (2011). Lessons from morpholino-based screening in zebrafish. *Briefings in Functional Genomics*, *10*(4), 181-188.

Berlato, C., Chan, K. V., Price, A. M., Canosa, M., Scibetta, A. G., & Hurst, H. C. (2011). Alternative *TFAP2A* isoforms have distinct activities in breast cancer. *Breast Cancer Research*, *13*(2).

Brewer, S., Feng, W., Huang, J., Sullivan, S., & Williams, T. (2004). Wnt1-Cre-mediated deletion of AP-2α causes multiple neural crest-related defects. *Developmental Biology*, *267*, 135-152.

Chambers, B.E., Gerlach, G.F., Clark, E.G., Chen, K.H., Levesque, A.E., Leshchiner, I., Goesling, W., & Wingert, R.A. (2019). *Tfap2a* is a novel gatekeeper of nephron diferentiation during kidney development. *Development*, *146*.

Darnell, D., Stanislaw, S., Kaur, S. & Antin P.B. (2010). Whole mount in situ hybridization detection of mRNAs using short LNA containing DNA oligonucleotide probes. *RNA - Cold Spring Harbor Laboratory Press*, *16*, 632 – 637.

Davuluri, R., Suzuki, Y., Sugano, S., Plass, C., & Huang, T.H.M. (2008). The functional consequences of alternative promoter use in mammalian genomes. *Trends in Genetics*, *24*(4), 167-177.

Eckert, D., Buhl, S., Weber, S., Jager, R, & Schorle, H. (2005). The AP-2 family of transcription factors. *Genome Biology*, *6*(246).

Kim, S., Carlson R., Zafreen, L., Rajpurohit, K., & Jagadeeswaran, P. (2009). Modular, easy-to-assemble, low-cost zebrafish facility. *Zebrafish, 6*, 269-274.

Knight, R.D., Javidan, Y., Zhang, T., Nelson, S., & Schilling, T. (2005). AP2-dependent signals from the ectoderm regulates craniofacial development in the zebrafish embryos. *Development*, *132*, 3127-3138.

Knight, R.D., Javidan, Y., Nelson, S., Zhang, T., & Schilling, T. (2004). Skeletal and pigment cell defects in the lockjaw mutant reveal multiple roles for zebrafish *tfap2a* in neural crest development. *Developmental Dynamics*, *229*, 87-98.

Knight, R.D., Nair, S., Nelson, S.S., Afshar, A., Javidan, Y., Geisler, R., Rauch, G.J., & Schilling, T.F. (2003). *Lockjaw* encodes a zebrafish *tfap2a* required for early neural crest development. *Development*, *130*, 5755-5768.

Limesand, S. and Anthony, RV. (2001). Novel activator protein-2α splice variants function as transactivators of the ovine placental lactogen gene. *European Journal of Biochemistry*, *268*, 2390 – 2401.

Mayor, R., and Theveneau, E. (2013). The neural crest. *Development*, *140*, 2247-2251.

Meier, P., Koedood, M., Philipp, J., Fontana, A., & Mitchell, P. J. (1995). Alternative mRNAs encode multiple isoforms of transcription factor AP-2 during murine embryogenesis. *Developmental Biology*, *169*, 1–14.

Mork, L., and Crump, G. (2015). Zebrafish craniofacial development: A window to early patterning. *Current Topics in Developmental Biology*, *115*, 235-269.

Nüsslein-Volhard, C. and Dahm, R. (2002) Zebrafish: a practical approach. New York: Oxford University Press. :303p

Ohtaka-Maruyama, C., Hanaoka, F., & Chepelinsky, A. (1998). A novel alternative spliced variant of the transcription factor *AP2a* is expressed in the murine ocular lens. *Developmental Biology*, *220,* 125 - 135

Schulte-Merker, S. and Stainier, DYR. (2014). Out with the old, in with the new: reassessing morpholino knockdowns in light of genome editing technology. *Development*, *141*, 3103 – 3104.

Stainier DYR, Raz E, Lawson ND, Ekker SC, Burdine RD, & Eisen JS, *et al.* (2017). Guidelines for morpholino use in zebrafish. *PLoS Genetics 13*(10): e1007000.

Theveneau, E., and Mayor, R. (2012). Neural crest delamination and migration: From epithelium-to-mesenchyme transition to collective migration. *Developmental Biology*, *366*, 34-54.

Walker, M.B, and Kimmel, C.B. (2007). A two-color acid free cartilage and bone stain for zebrafish larvae. *Biotechnic & Histochemistry*, 82:1, 23-28.

Williams, T., and Tijan, R. (1991a). Characterization of a dimerization motif in AP-2 and its function in heterologous DNA-binding proteins*. Science*, *251*, 1067-1071.

Williams, T., and Tijan, R. (1991b). Analysis of the DNA-binding and activation properties of the human transcription factor AP-2. *Genes Development*, *5*, 607-682.

Yunusov, D., Anderson, L., DaSilva, L.F., Wysocka, J., Ezashi, T., Roberts, R.M., & Verjovski-Almeida, S. (2016). *HIPSTR* and thousands of lncRNAs are heterogenously expressed in human embryos, primordial germ cells and stable cell lines. *Scientific Reports*, *6*(32753), 1-14.

Zhang, J., Hagopian-Donaldson, S., Serbedzija, G., Elsemore, J., Plehn-Dujowich, D., McMahon, A.P., Flavell, R.A., & Williams, T. (1996). Neural tube, skeletal and body wall defects in mice lacking transcription factor AP-2. *Nature*, *381*(6579), 238-241.